Al Azhar Bulletin of Science Vol. 29, No. 2 (December), 2018, pp. 13-18

BORATE GLASSES CONTAINING Bi, Na and Cu OXIDES as RADIATION SHIELDING MATERIALS

Sahar Abd El-Ghany

Department of Physic, Faculty of Science AL-Azhar University (Girls' Branch), Cairo, Egypt.

ABSTRACT

The basic gamma-ray shielding parameters such as mass attenuation coefficient, mean free path and effective atomic number of glass matrix with composition $0.45B_2O_3$. $0.1Na_2O$. $(0.1+x)Bi_2O_3$. $(0.35-x)CuO$ (x=0, 0.07, 0.14, 0.21, 0.28, 0.35) have been determined experimentally. The removal cross-section for fast neutrons is also calculated for the samples. The obtained results are correlated to their structural properties obtained from their infrared spectra.

Keywords: Bismuth borate glass, Radiation shielding parameters, Copper glass.

1. INTRODUCTION

The branch of radiation shielding materials has become very important in several important domains. It is well known that lead and concrete are the most commonly inexpensive shielding materials. The toxicity of lead, the variability in water content of concrete and non-transparency of both of them raise the necessity to develop better gamma-ray shielding materials [1]. In the recent years, there has been increasing interest in using glass materials as radiation shielding. Several researchers, have attempted to prepare lead free glasses [2-6]. It is observed that, for bismuth borosilicate glasses the mean free paths have lower values than the values of several types of standard shielding concretes [7,8]. Additionally, Marzouk et al., [9] observed that Bi_2O_3 borate glasses are not affected by continuous irradiation and can be considered as a very good shielding material. But, the main disadvantage of bismuth is the formation of metallic bismuth, which causes a deep coloration [10,11]. It is found that, the presence of CuO in the glass composition reduces its deep coloration and improves its optical properties. The addition of transition metals such as Cu is very important in memory switching devices [12] and non-linear optical devices applications [13]. While, the addition of sodium oxide is useful to provide low melting point of glass and expand the glass-forming region [14, 15].

The aim of the present work is to study the shielding parameters for gamma and neutrons radiations of produced glass systems to investigate the use of such glasses as radiation shielding material. Additionally, the aim is expanded to investigate the dependence of the structural properties of the present glass system on Bi_2O_3 concentrations by using Fourier Transform Infrared Spectroscopy (FTIR).

2. EXPERIMENTAL WORK

Glass batches of the system $0.45B_2O_3$. $0.1Na_2O$. $(0.1+x)Bi_2O_3$. $(0.35-x)CuO$ (x = 0, 0.07, 0.14, 0.21, 0.28, 0.35) were prepared by melt quenching technique. The H_3BO_3 and Na_2CO_3 were used as sources of B_2O_3 and Na_2O. The chemicals were mixed thoroughly and melted in porcelain crucible at 980^{o}C for 2 h. The glass samples were properly annealed at 350^{o}C. Then the annealing furnace was left to cool slowly to room temperature to avoid internal stress. The density of the samples was measured by Archimedes' principle using Tetracloride as immersion liquid.

The micro-hardness was measured at load 100 grams by a Vicker's diamond indentor tester (Leco AMH 100, USA).

The attenuation coefficient of gamma-ray was measured by a narrow beam transmission geometry by using 3″ x 3″ NaI(Tl) scintillation detector and radioactive sources ^{137}Cs and ^{60}Co having activities 9.5 μCi and 4.9 μCi

respectively. The counting time was chosen such that 10^3-10^5 counts were recorded under each photo peak.

The infrared absorption spectra of the glass samples were measured by using FTIR Perkin Elmer-Spectrum at room temperature in the range 400-4000 cm^{-1}.

3. RESULTS AND DISCUSSION

3.1 Density, molar volume and hardness

The density of the prepared glass can be calculated from the empirical relation,

$$\rho_{emp} = \sum_i w_i \rho_i \quad (1)$$

where w_i and ρ_i are the weight fraction and density of the oxide i in the glass sample respectively.

Accordingly, the empirical molar volume $(V_m)_{emp}$ was given by,

$$(V_m)_{emp} = M/\rho_{emp} \quad (2)$$

where M is the molecular weight of a glass sample. For experimental molar volume $(V_m)_{exp}$ replacing ρ_{emp} by ρ_{exp} in Eq. (2).

The study of glass density informs about any variation in the network structure of the glass. Additionally, the amorphous property of glasses can be confirmed by comparing the experimental and empirical values of both density and molar volume. Fig. 1 shows approximately linear increase in the density with increase of Bi_2O_3 and the empirical values of the density ρ_{emp} is higher than the experimental one, this gives an evidence for the pure glassy state of the prepared samples [16]. Moreover, Table 1 shows increase the molar volume with increase of Bi_2O_3 concentration and $(V_m)_{emp}$ is lower than $(V_m)_{exp}$, which confirm the amorphous nature of the present samples.

The increase in molar volume and density with increase of Bi_2O_3 content on the expense of CuO may be attributed to the difference in the molecular weights of CuO(Mw=79.55) and Bi_2O_3(Mw=466). This result agrees with Saudi et al., (2016) [17]. Also, Table (1) shows that there is a relative decrease of the hardness values (0.86-4.5%) with the replacement of CuO by Bi_2O_3, this may be due to the decrease of the covalence character of Bi-O than that of Cu-O.

Table 1. Chemical composition, molar volume and hardness of glass samples.

Sample No.	Composition (mol. %)				Molar volume (cm^3/mol.)		Hardness kg/mm^2
	B_2O_3	Na_2O	Bi_2O_3	CuO	$(V_m)_{exp}$	$(V_m)_{emp}$	
1	0.45	0.10	0.10	0.35	28.78	25.26	486.49
2	0.45	0.10	0.17	0.28	32.25	30.13	482.28
3	0.45	0.10	0.24	0.21	38.00	34.63	476.39
4	0.45	0.10	0.31	0.14	41.71	38.81	473.65
5	0.45	0.10	0.38	0.07	44.75	42.69	470.21
6	0.45	0.10	0.45	0	48.95	46.30	464.32

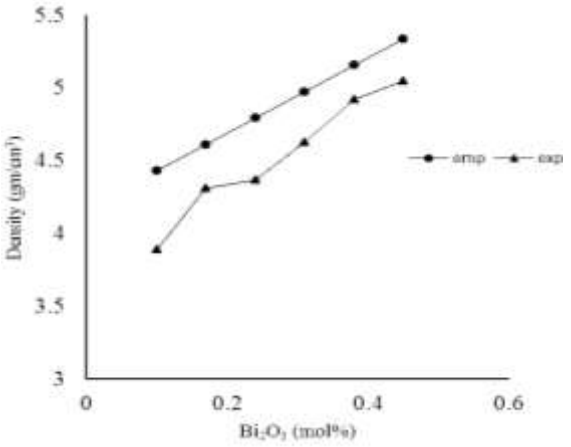

Fig. 1 The experimental and empirical density of the present glasses.

3.2 Theoretical aspect and experimental results for attenuation of gamma-ray

It is well known that the linear attenuation coefficient of a parallel beam of mono-energetic gamma-ray is calculated according to the Lambert–Beer law

$$I = I_o e^{-\mu t} \quad (3)$$

where I_o and I are the incident and transmitted intensities, t the thickness of the absorbing medium and μ is the linear attenuation coefficient. The experimental values of mass attenuation coefficient μ/ρ (cm^2/g) were compared with the theoretical values which were calculated by Win X com program [18]. Fig. 2 shows that the values of μ/ρ increase

with increasing the concentration of bismuth. This increase in mass attenuation coefficient is related to the increase in the density due to the formation of condensed structure of these glasses.

The mean free path (*MFP*) can be calculated as follows:

$$MFP = 1/\mu \qquad (4)$$

Fig. 3 shows that the *MFP* values of the glass samples decrease with increasing of bismuth concentration. It is well known that the *MFP* represents the average traveled distance between two successive photon collisions or interactions. So, the shorter *MFP* means more interaction of photons with the material and better shielding properties. This indicates that the glass system in the present work can be used as good radiation shielding materials.

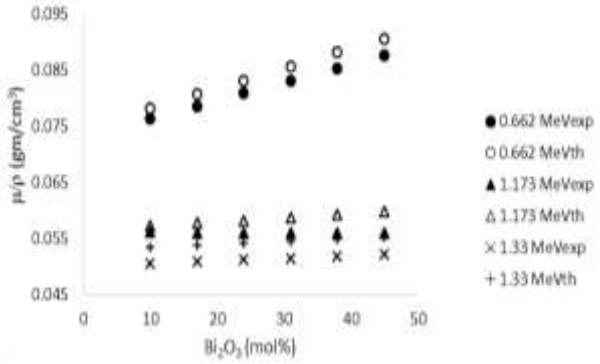

Fig. 2. The mass attenuation coefficient of the present glass samples at different energies.

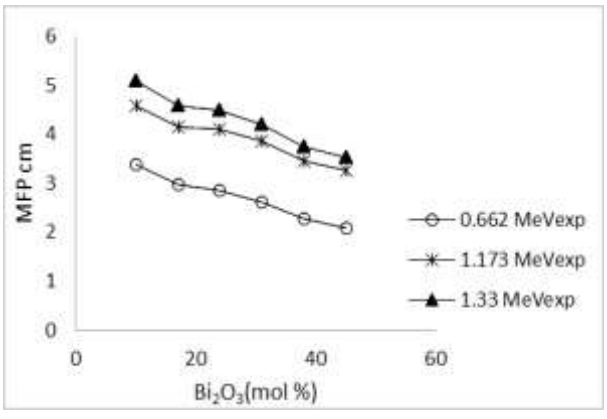

Fig. 3. The mean free path of the present glass samples at different energies.

By using the mass attenuation coefficient, the average atomic cross-section $\sigma_{t.a}$ can be calculated by using the following relation[19]:

$$\sigma_{t.a} = \left(\frac{\mu}{\rho}\right)\frac{M}{N_A}\frac{1}{\sum_i n_i} \qquad (5)$$

Where M is the molecular weight, N_A is the Avogadro's number and n_i is the number of formula units of ith element.

While the average electronic cross-section $\sigma_{t.el}$ is given by:

$$\sigma_{t.el} = \frac{1}{N_A}\sum \frac{f_i A_i}{Z_i}\left(\frac{\mu}{\rho}\right)_i \qquad (6)$$

where, A_i is the atomic weight of the i th element, Z_i its atomic number and $f_i \frac{n_i}{\sum_i n_i}$ is the fractional abundance of the i th element.

The effective atomic number (Z_{eff}) indicates that the gamma-ray attenuation in the material is related to the interaction of radiations with matter. The effective atomic number is given by:

$$Z_{eff} = \frac{\sigma_{t.a}}{\sigma_{t.el}} \qquad (7)$$

The variation of Z_{eff} as a function of photon energy in all samples is shown in Table 2. From this table, it can be seen that Z_{eff} increases with increasing the concentration of Bi_2O_3which indicates that there are more interactions of photons with the material that improve the shielding properties.

Table 2. Effective atomic number Z_{eff} of the present glass samples.

Bi_2O_3 (mol %)	0.662 MeV		1.173 MeV		1.33 MeV	
	Experiment	Theory	Experiment	Theory	Experiment	Theory
0.1	14.02	14.37	10.30	10.51	9.27	9.81
0.17	16.53	16.96	11.79	12.14	10.69	11.31
0.24	18.85	19.39	13.07	13.57	11.93	12.62
0.31	21.03	21.68	14.18	14.86	13.03	13.80
0.38	23.09	23.86	15.16	16.03	14.03	14.83
0.45	25.06	25.92	16.03	17.09	14.93	15.80

3.3 The neutron removal cross-section (Σ_R)

There are some accurate empirical expressions for calculation of the mass removal cross-section $(\Sigma_R/\rho)_e$ for any element e were given in Wood [20]. For a compound C which

consistent of l elements, the mass removal cross-section $(\sum_R/\rho)_c$ (in cm^2g^{-1}) is given by [21]:

$$\left(\sum_R/\rho\right)_c = \sum_{e=1}^{l} R_e \left(\sum_R/\rho\right)_e \qquad (8)$$

where R_e is the mass fraction of the element e in the compound c. While, the removal cross-section $\sum_{RS}$ (cm^{-1}) for a sample that has n compounds will be given by [21]:

$$\sum_{RS} = \sum_{c=1}^{n} (F_W)_c \rho_s \left(\sum_R/\rho\right)_c \qquad (9)$$

where $(F_w)_c$ is the weight fraction of the compound c and ρ_s is the density of the sample. Table 3 shows that there is a relative decrease (1-5.6%) in the values of $\sum_{RS}$ as the concentration of Bi_2O_3 increases. This is due to the difference between $(\sum_R/\rho)$ of Bi_2O_3(.0134 cm^2g^{-1}) and $(\sum_R/\rho)$ of CuO (0.0239 cm^2g^{-1}).

Table 3. The manual calculated removal cross-section $\sum_{RS}$ (cm^{-1}) for glass samples.

Bi_2O_3 (mol %)	$\sum_{RS}$ (cm^{-1})
0.1	0.117
0.17	0.116
0.24	0.114
0.31	0.113
0.38	0.112
0.45	0.110

3.4 IR results

The infrared spectra of the studied glass samples are displayed in Fig. 4, which shows that the band profile of the samples is nearly similar, but there is a systematic change in the relative intensities as CuO is replaced by Bi_2O_3. For a quantitative analysis of the IR spectra, the deconvolution method was carried out for the absorption profiles using the "peak fit" program applying the Gaussian band shapes. The deconvolution data has been represented in Table 4. An example of a deconvolution spectra for sample 4 is illustrated in Fig. 5, which shows that the band centered at~500 cm^{-1} represents the characteristic stretching band of Bi-O bonds in BiO_6 octahedral units. This result agrees with Dimitrov et al., and Iordanova et al., [22, 23]. The aforementioned band lies on the same position of B-O-B bond bending vibration [24-26]. Fig. (6 a) shows that the relative intensity of this band increases as the concentration of Bi_2O_3 increases up to about 0.31 mol.% and then the relative intensity decreases. This behavior may be due to the replacement of CuO by Bi_2O_3 where the structure is affected by the magnetic properties of Cu^{2+} [27].

The band at ~ 700 cm^{-1} is attributed to both Bi-O bonds in BiO_3 pyramid and O_3B-O-BO_3 bending vibrations [26,28,29]. The relative intensity of this band increases as the concentration of Bi_2O_3 increases up to 0.31 mol% and then the relative intensity decreases with increasing Bi_2O_3 concentration as shown in Fig. (6 a).

Table 4. IR deconvolution data for the glass samples.

Sample No.	Bi_2O_3 (mol. %)	Relative intensity			
		λ (400-500) cm^{-1}	λ (500-700) cm^{-1}	BO_4 λ (800-1200) cm^{-1}	BO_3 λ (1200-1500) cm^{-1}
1	0.10	0.078	0.022	0.348	0.550
2	0.17	0.062	0.024	0.393	0.521
3	0.24	0.096	0.025	0.357	0.520
4	0.31	0.102	0.029	0.408	0.460
5	0.38	0.090	0.025	0.359	0.470
6	0.45	0.065	0.017	0.441	0.474

The behavior of the band region from 800 to 1200 cm^{-1} is shown in Fig. (6 b), this band is related to the vibration of B-O in BO_4 groups. It is obvious that the relative intensity of this band increases as the concentration of Bi_2O_3 increases on the expense of CuO. In contrast, the relative intensity which is related to the stretching vibration of B-O in BO_3 groups in the region from 1200-1500 cm^{-1} is found to decrease as Bi_2O_3 concentration increases. Both the increase in BO_4 relative intensity and the decrease of BO_3 relative intensity which represent the conversion of BO_3 groups into BO_4 groups may be due to the increase of the number oxygen atoms as the Bi_2O_3 concentration is increased on the expense of CuO. The increase of the BO_4 which is denser than BO_3 leads to increase the density of the prepared samples. The decrease of BO_3 reduces the strength of the bonds which agrees with the decrease of the hardness values.

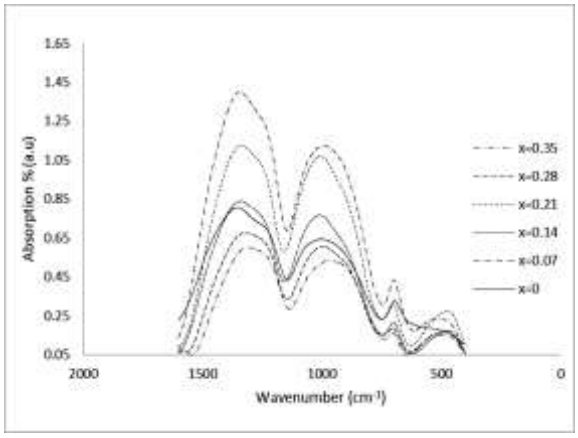

Fig. 4. Infrared absorption spectra of the 0.45 B_2O_3. 0.1Na_2O. (0.1+*x*) Bi_2O_3. (0.35-*x*) CuO (0≤*x*≤ 0.35) glasses.

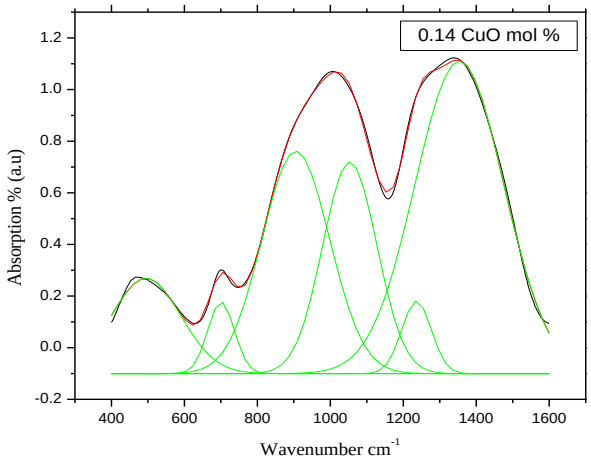

Fig. 5. The deconvolution spectra of the sample 4.

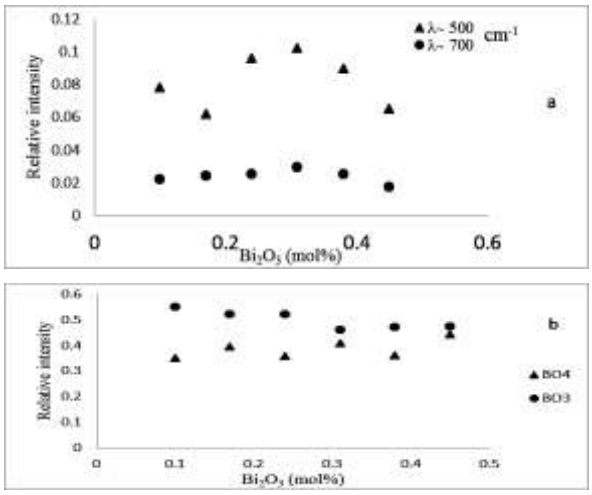

Fig. 6. IR deconvolution data for the 0.45 B_2O_3. 0.1Na_2O. (0.1+*x*) Bi_2O_3. (0.35-*x*) CuO (0≤*x*≤ 0.35) glasses.

CONCLUSION

In the present work, the radiation shielding and some other properties of borate glasses containing Na, Bi and Cu oxides have been investigated. The amorphous property of the samples was confirmed by comparing the experimental and the empirical values of both density and molar volume. It is observed that the values of μ/ρ increase with increasing the concentration of Bi_2O_3. From the FTIR analysis, there are small relative decrease of hardness values (0.86-4.5%) related to decrease of bonds because of decrease of BO_3 with increase of the Bi_2O_3 concentration.

The results of this work indicated that the present glass system can be considered as suitable shielding materials for gamma rays and neutrons.

REFERENCES

1. C.M. Lee, Y.H. Lee, K.J. Lee, Prog. Nucl. Energy 49 (2007) 303.
2. K. Singh, H. Singh, G. Sharma, L. Gerward, A. Khanna, R. Kumar, R. Nathuram, H. S. Singh, Radiat. Phys. Chem. 72 (2005) 225.
3. K. Kaur, K. J. Singh, V. Anand, Radiation Physics and Chemistry120 (2016) 63.
4. Reza Bagheri, Alireza Khorrami Moghaddam, and Hassan Yousefnia, Nuclear Engineering and Technology (2017) 216.
5. B.O. El-bashir, M.I. Sayyed, M.H.M. Zaid, K.A. Matori, Journal of Non-Crystalline Solids (2017) 92.
6. N. Singh, K. J. Singh, K. Singh, H. Singh, Nucl. Instrum. Methods Phys. Res. Sect. B: Beam Interact. Mater. Atoms (2004) 305.
7. N. Chanthima, J. Kaewkhao, Annals of Nuclear Energy (2013) 23.
8. Kulwinder Kaur, K.J. Singh, Vikas Anand, Nuclear Engineering and Design (2015) 31.
9. M. A. Marzouk, F. H. ElBatal, W. H. Eisa, N. A. Ghoneim, J. Non-Cryst. Solids (2014) 155.
10. O. Sanz, E. Haro-Poniatowski, J. Gonzalo, M.F. Navarro, Journal of Non- Crystalline Solids (2006) 761.

11. Y. Zhang, Y. Yang, J. Zheng, W. Hua, G. Chen, Journal of the American Ceramic Society (2008) 3410.

12. L. Baia, R. Stefan, W. Kiefer, J. Popp, S. Simon, Journal of Non-Crystalline Solids (2002) 379.

13. A. Lin, B. H. Kim, D. S. Moon, Y. Chung, W. T. Han, Optics Express (2007) 3665.

14. F. H. ElBatal, M. S. Selim, S. Y. Marzouk, M. A. Azooz, Phys. B: Condens. Matter (2007) 126.

15. P. Limkitjaroenporn, J. Kaewkhao, P. Limsuwan, W. Chewpraditkul, J. Phys. Chem. Solids (2011) 245.

16. A.M. Zoulfakar, A.M. Abdel-Ghany, T.Z. Abou-Elnasr, A.G. Mostafa, S.M. Salem, H.H. El-Bahnaswy, Applied Radiation and Isotopes (2017) 269.

17. H. A. Saudi, M. A. Samei, N. M. Ebrahem and W. M. El-Meligy, Global Journal of Physics 3 (2016) 204, www.gpcpublishing.com.

18. L. Gerward, N. Guilbert, K. B. Jensen, H. Levring, Radiat. Phys. Chem. (2004) 653.

19. Sukhpal Singh, Ashok Kumar, Devinder Singh, Kulwant Singh Thind , Gurmel S. Mudahar, Nuclear Istruments and Methods in Physics Research B 266 (2008) 140.

20. J. Wood, Computational Methods in Reactor Shielding. Pergamon Press, Inc., New York, USA. (1982).

21. A.M. El-Khayatt, Annals of Nuclear Energy 37 (2010) 218.

22. V. Dimitrov, Y. Dimitriev, A. Montenero, J. Non–Cryst. Solids 180 (1994) 51.

23. R. Iordanova, Y. Dimitriev, V. Dimitrov, S. Kassabov, D. Klissurski, J. Non-Cryst. Solids 204 (1996) 141.

24. E.I. Kamitsos, M.A. Karakassides, Phys. Chem. Glasses 30 (1989) 19.

25. E.I. Kamitsos, M.A. Karakassides, G.D. Cryssikos, J. Phys. Chem. 91 (1987) 1073.

26. G. Fuxi, Optical and Spectroscopic Properties of Glass, Springer, Berlin (1991).

27. I. Ardelean, Simona Cora, Dorina Rusu, Physica B 403 (2008) 3682.

28. A. Bishay, C. Maghrabi, Phys. Chem. Glasses 10 (1969) 1.

29. S.G. Motka, S.P. Yawale, S.S. Yawale, Bull. Mater. Sci. 25 (2002)